

Magnetic field modulation spectroscopy of rubidium atoms

S PRADHAN*, R BEHERA and A K DAS

Laser and Plasma Technology Division, Bhabha Atomic Research Centre, Trombay,
Mumbai 400 085, India

*Corresponding author. E-mail: spradhan@barc.gov.in

MS received 13 July 2011; revised 17 October 2011; accepted 8 November 2011

Abstract. The magnetically modulated saturation absorption profile is studied for a wide range of external DC magnetic field. The salient features of Doppler-free signal generated by laser frequency modulation and atomic energy level modulation are compared. The DC offset of the signal profile is found to be unstable as the external DC magnetic field is changed. The technical difficulty of tuning laser frequency under locked condition over a large frequency span is discussed along with possible solutions.

Keywords. Modulation spectroscopy; saturation absorption spectroscopy; Zeeman splitting.

PACS Nos 42.62.Fi; 32.60.+j; 33.55.+b

1. Introduction

The various laser spectroscopic techniques are vital components of experiments used to study atomic properties [1,2]. The frequency modulation spectroscopy (FMS) is a powerful technique, where the imposed frequency modulation is essentially converted into an amplitude modulation as an atomic transition is encountered [3]. The FMS can easily circumvent the usual problem of laser intensity fluctuation and offer en suite phase-sensitive detection of the signal, thereby paving the way for very high sensitive measurement in the parts per billion (PPB) levels [4]. On the other hand, the saturation FMS (SFMS) can be used as a very precise frequency reference in experiments involving laser-cooled atoms, frequency standards as in atomic clock, coherent laser spectroscopy etc. The SFMS is an extension to the FMS, where the laser frequency is modulated in a saturation spectroscopy set-up and the signal is extracted by demodulating the output in reference to the modulation frequency. Thus, in an SFMS the sub-Doppler features of the saturation spectroscopy is preserved, at the same time a derivative signal is generated at the atomic line centre for the easy operation of the servo-loop as required for frequency stabilization. The SFMS can be further integrated using the technique of magnetic field-induced tuning of the saturation profile [5,6], thereby paving the way for easy tuning of

the locked laser frequency. This technique can be a less expensive substitute for the offset beat frequency locking. It may be noted that unlike offset beat frequency, this technique requires neither frequency stabilized reference light source nor high speed detector.

The operation of the FMS can be classified into two regimes depending on the modulation depth and frequency. It is termed as wavelength modulation (WM) when modulation depth is very large but modulation frequency is smaller compared to the characteristic width of the signal (typically <1 MHz). On the other hand, it is called frequency modulation (FM) when the modulation depth is smaller but the frequency larger (larger than the width of the signal, >10 MHz for sub-Doppler spectroscopy). However, the physical origin of the WM and FM are quite similar [7] and are generally referred to as FMS. In this paper, we have studied the SFMS in the presence of magnetic field for σ^+ circularly polarized pump and probe laser beam in the wavelength modulation regime. The modulation of the diode laser wavelength can be done either by the modulation of injection current or modulation of the voltage fed to the piezoactuator. The former offers relatively high-frequency modulation, whereas the latter is advantageous for reducing spurious intensity modulation [8]. Here, the SFMS signal is generated by modulating the piezoactuator voltage resulting in the modulation of the wavelength of the laser beam. However, in many experiments, part of the beam is used for frequency stabilization and the rest of the beam is used for main experimental system. The modulation of the piezoactuator voltage (or diode laser current) generates a frequency-modulated beam as required for generating FMS signal, at the same time the main laser beam also gets modulated undesirably. This can be circumvented using an acousto-optic modulator (AOM) or an electro-optic modulator (EOM) in the path of the laser beam used for frequency stabilization [9,10]. The alternative way of generating a derivative signal using a technique known as dichroic atomic vapour laser lock (DAVLL), which uses differential Doppler-limited absorption rates of the σ^+ and σ^- polarized light beam in the presence of a DC magnetic field is reported in [11]. This technique has been subsequently extended to the Doppler-free configuration [12]. One of the important advantages of the DAVLL-based technique is that it does not require any laser frequency modulation.

In this work, the atomic Zeeman level is modulated by an oscillating magnetic field to generate the derivative profile at the line centre and subsequently shifted by applying a DC magnetic field [13,14]. We compare the magnetic field modulation saturation signal with the piezoactuator-modulated FMS signal for a wide range of magnetic field. The salient features of magnetically-modulated saturation signal are discussed. In ref. [13], the laser frequency stability of the magnetic field-modulated signal has been studied using Allan variance and heterodyne beat frequency. In the present work, we have discussed the technical difficulties of tuning the laser under lock to the magnetic field modulation signal. The various possibilities for compensating undesirable DC offset arising in the magnetically-modulated signal are presented.

2. Experimental set-up

The schematic of the experimental set-up is shown in figure 1. It essentially consists of two saturation absorption spectroscopy (SAS) set-up. One of the SAS set-up is used for frequency calibration and is termed as the reference SAS set-up. The other SAS set-up

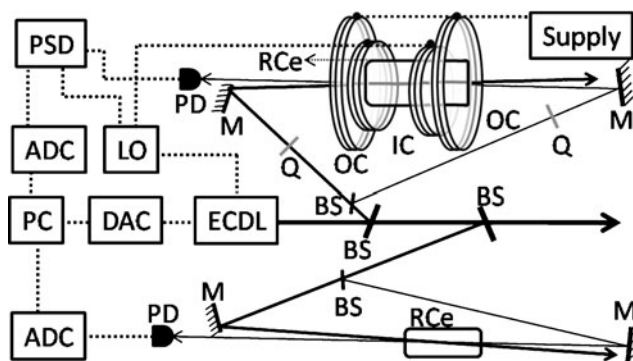


Figure 1. Schematic diagram of the experimental set-up. It essentially consists of two saturation absorption set-up. The atomic vapour cell in the upper saturation absorption set-up is placed inside two pairs of electromagnets for providing a bias and modulation magnetic field. The pump and probe laser beams are right circularly polarized in the upper set-up. The lower saturation absorption set-up is used as a frequency reference. ECDL: external cavity diode laser, PC: personal computer, DAC: digital-to-analog converter, ADC: analog-to-digital converter, LO: local oscillator, PSD: phase-sensitive detector, PD: photodiode, Q: quarter wave plate, BS: 10% R beam splitter, M: mirror, RCe: rubidium vapour cell, OC: outer coil, IC: inner coil, supply: current supply for outer coil.

is used for FM spectroscopy. Here, the atomic vapour cell is placed inside two pairs of coils for producing a homogeneous DC magnetic field and a modulating magnetic field. The outer pair of the coil in Helmholtz configuration has an internal diameter of 70 mm each and is placed 15 mm apart. This outer pair of coils is used to generate a DC near-homogeneous magnetic field inside the rubidium atomic vapour cell. We had to adopt this configuration instead of a solenoid due to the constraint arising from the geometry of the atomic vapour cell. There is also an additional inner pair of coils placed in between the outer coil and the atomic vapour cell. This pair of coils is also in Helmholtz configuration and used to produce modulation in the magnetic field. We prefer to use this additional pair of coils, instead of adding an oscillating current to the outer coil as it offers flexibility in the design of the coils for applying higher frequency modulation. All these electromagnets are homemade and do not require any precise equipment for fabrication. The atomic vapour cell has a length of ~ 3.5 cm and is free from buffer gas. It contains natural isotope composition of rubidium atoms at a residual vacuum of 10^{-6} Torr. The pump and the probe beams are made right circularly polarized using quarter-wave plates in their respective path and pass through the rubidium vapour cell in almost overlapping, counter-propagating direction. The transmission of the probe laser beam through the vapour cell is monitored by a pin photodiode. The pump (probe) laser beam has a power of $760 \mu\text{W}$ ($50 \mu\text{W}$) with a beam size of roughly $3 \text{ mm} \times 1 \text{ mm}$. The diode laser is tuned to the 780 nm rubidium D2 line. The FMS signal is generated by the modulation of the piezoactuator voltage and the magnetically-modulated saturation signal is generated by the modulation of external magnetic field, thereby modulating the laser frequency or the atomic energy level respectively. The output voltage from the local oscillator in figure 1 is added with the piezoactuator voltage, resulting in the modulation of the laser

wavelength. For the experiments involving magnetically-modulated saturation signal, the output of the local oscillator is used for supplying oscillating current in the inner coils. In both piezoactuator modulation SFMS and magnetic field modulation saturation signals, the output of the photodetector is phase-sensitively detected at the applied modulation frequency using a lock-in amplifier.

3. Results and discussions

It has been established that the atomic resonances in SAS can be shifted in a control manner by applying a DC magnetic field [5,6]. This allows generation of reference signal away from the atomic transition frequency. Thus it is possible to lock the laser frequency to the side of an atomic resonance and scan the laser frequency under locked condition by changing the applied DC magnetic field. However, locking to the side of the resonance results in non-linear scanning of the laser frequency as a function of magnetic field [6]. This can be circumvented by stabilizing the laser frequency on the peak of the atomic transition. The error signal at the peak of an atomic transition line is achieved by the FMS, where laser frequency is modulated and the signal is phase-sensitively detected at the

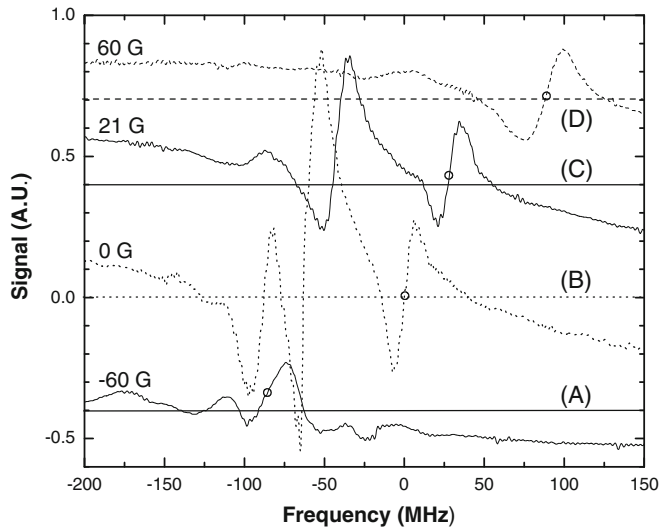


Figure 2. FM spectroscopy using piezoactuator modulation to induce modulation in the laser frequency. The peak frequency deviation and modulation frequency are 30 MHz and 100 Hz respectively. The horizontal axis represents the detuning of the laser frequency relative to the centre of the $5s_{1/2}F = 3 \rightarrow 5p_{3/2}F' = 4$ transition at zero magnetic field. The plots at various magnetic fields are shifted for better illustration. The straight horizontal lines (A), (B), (C) and (D) represent the DC offset values corresponding to the signal for -60 G, 0 G, 21 G and 60 G respectively. The DC offset values are extracted from the value of the signal at far-off resonant frequency taken at zero magnetic field value. The circle in each curve marks the centre of the $5s_{1/2}F = 3 \rightarrow 5p_{3/2}F' = 4$ hyperfine transition of the ^{85}Rb atoms.

modulation frequency. The SFMS signals generated by the modulation of the piezoactuator voltage are illustrated in figure 2. The amplitude and position of the resonances appearing in the SFMS profile are observed to be effected by various degrees with respect to the applied magnetic field. The overall behaviour of the profile primarily depends on the magnetic moment of the involved states and the details of the optical pumping mechanism. For simplicity we shall only discuss about the $5s_{1/2}F=3 \rightarrow 5p_{3/2}F'=4$ transition of the ^{85}Rb D2 line. The peak position of the signal appears with a slope in the derivative of the signal and is marked by an open circle in figure 2. The nearest turnover to this point lies at a separation of ~ 13 MHz and corresponds to the width of the signal. The amplitude of the signal can be extracted from the difference of the signal level between the two turnover points. As the magnetic field is increased, the $5s_{1/2}F=3 \rightarrow 5p_{3/2}F'=4$ transition is observed to be shifting monotonically to the higher frequency side. This is consistent with the reported work, where it has been pointed out that the signal has major contribution from the $5s_{1/2}F=3, m_f=+3 \rightarrow 5p_{3/2}F'=4, m_{f'}=+4$ transition owing to the optical pumping to the stretched state in $\sigma^+ - \sigma^+$ pump-probe configuration [5,6]. Similar kind of derivative signal generated from the magnetic field modulation saturation spectroscopy is illustrated in figure 3. The similarities and differences in the

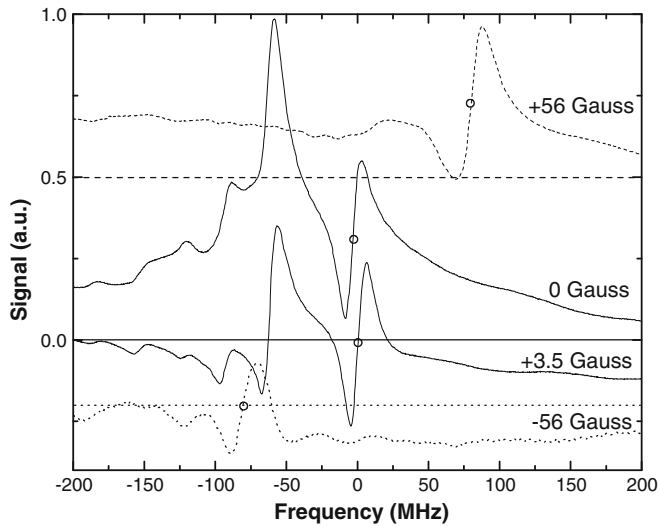


Figure 3. FM spectroscopy using magnetic modulation to induce modulation in the atomic energy level. The amplitude and frequency of magnetic field modulation are 6.7 G and 100 Hz respectively. The plots corresponding to ± 56 G are shifted for better illustration. The straight horizontal solid line represents the DC offset value for the spectrum corresponding to 0 G and 3.5 G. The dotted and dashed lines correspond to the DC offset values for the curves representing -56 G and $+56$ G respectively. The DC offset values are extracted from the value of the signal at far-off resonant frequency taken at zero magnetic field value. The circle in each curve marks the centre of the $5s_{1/2}F=3 \rightarrow 5p_{3/2}F'=4$ hyperfine transition of the ^{85}Rb atoms. It may be noted that the intensity corresponding to the centre of the $5s_{1/2}F=3 \rightarrow 5p_{3/2}F'=4$ transition changes with respect to the DC offset value depending on the magnetic field.

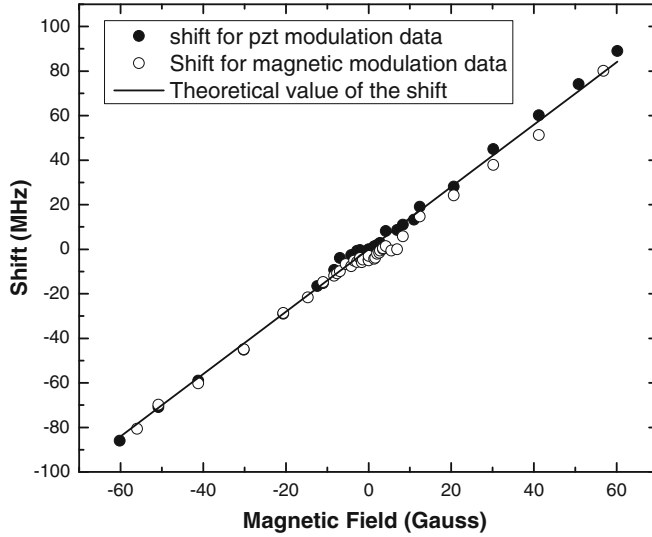


Figure 4. Shift of the $5s_{1/2}F = 3 \rightarrow 5p_{3/2}F' = 4$ transition line of ^{85}Rb . The experimental data obtained from modulation of the magnetic field (PZT voltage) are represented by the open (solid) circle. For the magnetic field modulation data, the amplitude and frequency of modulation are 6.7 G and 100 Hz respectively. The solid line shows the expected theoretical line with a slope of +1.4 MHz/G.

piezovoltage-modulated SFMS signal and magnetic field-modulated saturation signal are discussed in the following section.

The shift in the centre of $5s_{1/2}F = 3$, $m_f = +3 \rightarrow 5p_{3/2}F' = 4$, $m_{f'} = +4$ transition as a function of magnetic field obtained by piezoactuator voltage and magnetic field modulation are shown in figure 4. As defined earlier, the centre of $5s_{1/2}F = 3$, $m_f = +3 \rightarrow 5p_{3/2}F' = 4$, $m_{f'} = +4$ transition is taken as the middle of the two turnovers, marked by circles in figures 2 and 3. The frequency shift as a function of magnetic field obtained from both of these techniques are found to be consistent with the results obtained from the shift of the SAS lines and follows close with the theoretical slope of +1.4 MHz/Gauss [5]. The linear shift of the line centre with the applied magnetic field offers analogous tuning of the laser frequency locked to the centre of $5s_{1/2}F = 3$, $m_f = +3 \rightarrow 5p_{3/2}F' = 4$, $m_{f'} = +4$ transition. However, such a possibility also depends on the stability of the DC offset of $5s_{1/2}F = 3$, $m_f = +3 \rightarrow 5p_{3/2}F' = 4$, $m_{f'} = +4$ transition with respect to the applied magnetic field. The DC offset is defined as the difference in signal level between the centre of the derivative profile of the concerned transition and signal at the far-off resonant position. Although the shift in the position of the signal is linear with respect to the applied magnetic field, the linearity of the locked laser frequency will be ruined if the DC offset is not stable. If the change in the DC offset is less than half of the signal amplitude, the laser can still be tuned under locked condition though the tuning will not be linear with the applied magnetic field. For the DC offset changing larger than half of the signal amplitude, the frequency tuning of the laser under locked condition will not be feasible as the lock point will move out of the capture range. Although continuous tuning will not be possible, it may be noted that it is still possible to lock the laser at any value of magnetic field

by changing the value of lock set point. Thus tuning of the laser frequency under locked condition will require simultaneous correction in the lock set point along with the change in the applied magnetic field.

The DC offset of the $5s_{1/2}F = 3, m_f = +3 \rightarrow 5p_{3/2}F' = 4, m_{f'} = +4$ transition centre as function of applied magnetic field obtained from piezoactuator voltage and magnetic field modulation is shown in figure 5. The DC offset of the magnetic field modulation signal exhibit a derivative profile near zero magnetic field. The DC offset of the piezoactuator voltage-modulated signal also shows similar behaviour with much smaller amplitude. It is worth noting that the primary interest for laser frequency stabilization will be the relative DC offset, which can be defined as the ratio of the DC offset to half of the corresponding signal amplitude. The capture range for laser frequency stabilization along with the relative DC offset is shown in the inset of figure 5. From this it is evident that even for piezoactuator-modulated SFMS signal, the tuning of the laser frequency under locked condition will not be linear with the magnetic field. In fact, the laser is expected to go out of lock for certain interval of the applied magnetic field.

The change in the DC offset for piezoactuator voltage and magnetic field modulation spectroscopy as a function of magnetic field is surprising. Such a behaviour can arise from the conventional Faraday rotation observed in the presence of static magnetic field [15]. However, in our experiments we have not used any polarization filter, where the

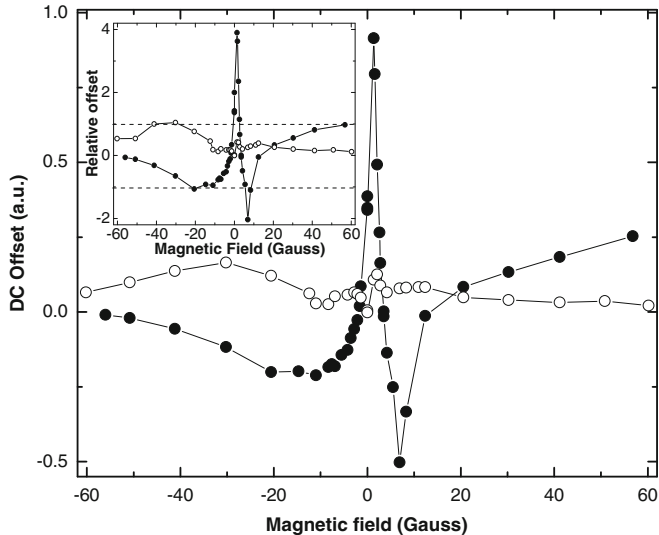


Figure 5. Shift of the $5s_{1/2}F = 3 \rightarrow 5p_{3/2}F' = 4$ line centre of the ^{85}Rb atoms from the DC offset value as a function of the applied magnetic field. The data obtained from the piezoactuator-modulated SFMS (magnetic field-modulated saturation signal) is represented by the open (solid) circle. For the magnetic field modulation data, the amplitude and frequency of modulation are 6.7 G and 100 Hz respectively. The inset represents the ratio of the DC offset to half of the corresponding signal amplitude with the symbols maintaining identity. The horizontal dashed lines in the inset marks the boundary for the relative DC offset, where the lock point is within the capture range.

Faraday effect can contribute to the signal profile. It has been established that optical pumping among the Zeeman substate and between the hyperfine levels significantly alters the saturation absorption profiles [6]. The observed change in the DC offset can arise from such optical pumping processes among the Zeeman substate. As the optical pumping is associated with characteristic time-scale, the change in the DC offset is expected to vary with the amplitude and frequency of modulation. In the following part, the parametric dependences of the DC offset arising in the magnetic modulation SAS profiles are discussed.

The change in the DC offset and amplitude of $5s_{1/2}F = 3, m_f = +3 \rightarrow 5p_{3/2}F' = 4, m_{f'} = +4$ transition as a function of the magnetic field modulation frequency is shown in figure 6. Both the DC offset and the signal amplitude are found to be maximized for a modulation frequency of ~ 62 Hz. However, the DC offset and the amplitude behave distinctively as the modulation field amplitude is varied (please see figure 7). The amplitude is found to be increasing linearly up to the modulation magnetic field amplitude of ~ 8 G, thereafter attains a nearly saturation value on further increase in the amplitude of the modulation field. Interestingly the DC offset is nearly constant up to a modulation amplitude of ~ 8 G and falls linearly on further increase in the amplitude of the modulation field. The DC offset is found to be crossing the zero offset value for an applied magnetic field modulation of ~ 15 G. In fact, we have observed that the DC offset can be compensated by changing the modulation amplitude at any desired magnetic field value. The compensation of the DC offset at different external magnetic field value requires different amplitude of the modulation field. Thus, it is possible to realize

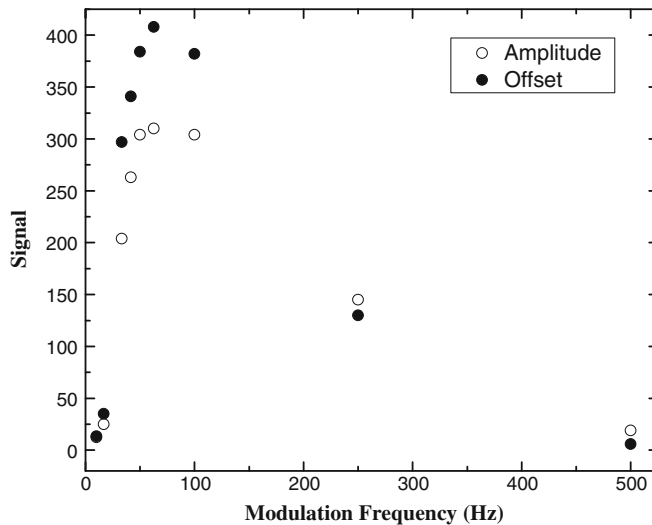


Figure 6. The dependence of the amplitude of the magnetic field modulated saturation signal for $5s_{1/2}F = 3 \rightarrow 5p_{3/2}F' = 4$ transition (open circle) and corresponding shift of the line centre from the DC offset value as a function of the modulation frequency. Both of these parameters are found to be maximized for the modulation frequency of ~ 62 Hz. The experimental data correspond to the modulation amplitude of 3.4 G at zero DC magnetic fields.

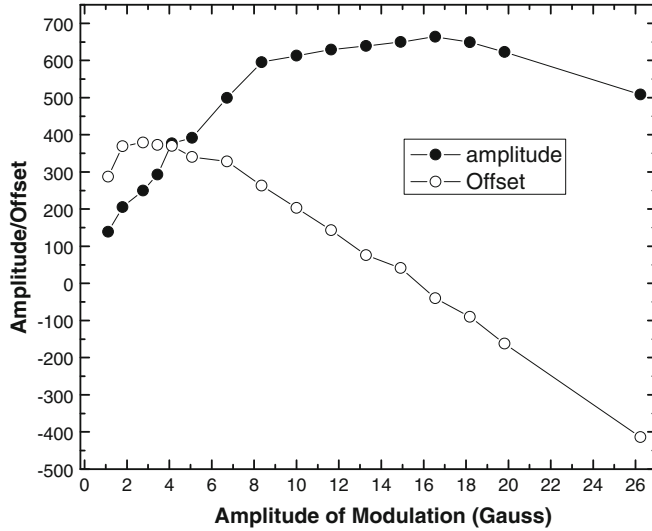


Figure 7. The variation in the amplitude of the magnetic field modulated saturation signal for $5s_{1/2}F = 3 \rightarrow 5p_{3/2}F' = 4$ transition (open circle) along with the corresponding shift of the line centre from the DC offset value is plotted against the amplitude of the modulation field. The experimental data correspond to the modulation frequency of 100 Hz at zero DC magnetic fields. The amplitude of the signal attains a plateau for magnetic modulation fields larger than ~ 8 G. On the contrary, the shift of the line centre from DC offset value falls linearly beyond this value and crosses the zero value for a modulation amplitude of ~ 15 G.

continuous tuning of laser frequency locked on the derivative signal obtained from magnetic field modulation by simultaneously changing the amplitude of modulation. There are several other possibilities for compensating the DC offset, like demodulation at higher (third or above) harmonics, adjustment of the reference phase of the lock-in demodulator, balanced detection etc. [16,17] and the implementation of this technique needs further investigation.

4. Conclusions

The experimental technique for generating derivative signals using piezomodulated FM spectroscopy and magnetic field modulation signal are compared. The latter technique is advantageous for experiments requiring modulation-free frequency-stabilized laser beams. The possibilities of tuning the laser frequency under locked condition using the magnetic field modulation are discussed. This can be achieved by compensating the DC offset by adjusting lock set point or changing the amplitude of the modulation field.

Acknowledgement

The authors are thankful to Dr L M Gantayet, Director, Beam Technology Development Group for his support and keen interest in this research work.

References

- [1] C J Foot, *Atomic physics*, Oxford master series in atomic, optical and laser physics (Oxford University Press, 2005)
- [2] W Demtroder, *Laser spectroscopy: Basic concepts and instrumentation* (Springer International Edition, 2004)
- [3] G C Bjorklund, M D Levenson, W Lenth and C Ortiz, *Appl. Phys.* **B32**, 145 (1983)
- [4] K P Petrov *et al*, *Appl. Phys.* **B64**, 567 (1997)
- [5] T P Dinneen, C D Wallace and P L Gould, *Opt. Comm.* **92**, 277 (1992)
- [6] S Pradhan and B N Jagatap, *J. Opt. Soc. Am.* **B28**, 398 (2011)
- [7] J M Supplee, E A Whittker and W Lenth, *Appl. Opt.* **33**, 6294 (1994)
- [8] M Vainio, M Merimaa and K Nyholm, *Opt. Comm.* **267**, 455 (2006)
- [9] V N Baryshev, Yu S Domnin and L N Kopylov, *Quantum Electron.* **37**, 1006 (2007)
- [10] T Mitsui, K Yamashita and K Sakurai, *Appl. Opt.* **36**, 5494 (1997)
- [11] K L Corwin, Z-T Lu, C F Hand, R J Epstein and C E Wieman, *Appl. Opt.* **37**, 3295 (1998)
- [12] V B Tiwari, S Singh, S R Mishra, H S Rawat and S C Mehendale, *Appl. Phys.* **B83**, 93 (2006)
- [13] T Ikegami, S Oshima and M Ohtsu, *Jpn. J. Appl. Phys.* **28**, L1839 (1989)
- [14] S Lecomte, E Fretel, G Mileti and P Thomann, *Appl. Opt.* **39**, 1426 (2000)
- [15] G Labeyrie, C Miniatura and R Kaiser, *Phys. Rev.* **A64**, 033402 (2001)
- [16] S Schilt, L Thévenaz and P Robert, *Appl. Opt.* **42**, 6728 (2003)
- [17] R Matthey, S Schilt, D Werner, C Affoldberbach, L Thévenaz and G Mileti, *Appl. Phys.* **B85**, 477 (2006)